A management tool for estimating bioenergy production and carbon sequestration in *Eucalyptus globulus* and *Eucalyptus nitens* grown as short rotation woody crops in north-west Spain

César Pérez-Cruzado[1,3,*], Agustín Merino[1,2], Roque Rodríguez-Soalleiro[1,3]

[1]Unit of Sustainable Forest Management, University of Santiago de Compostela,

[2]Soil Science and Agricultural Chemistry Department, University of Santiago de Compostela,

[3]Crop Production Department, University of Santiago de Compostela,

E-27002 Lugo, Spain

* Corresponding author. Tel.: (+34) 982 285900 Ext 23108; fax: (+34) 982 285926

E-mail address: cesar.cruzado@usc.es

A management tool for estimating bioenergy production and carbon sequestration in *Eucalyptus globulus* and *Eucalyptus nitens* grown as short rotation woody crops in north-west Spain

César Pérez-Cruzado[1,3,*], Agustín Merino[1,2], Roque Rodríguez-Soalleiro[1,3]

[1]Unit of Sustainable Forest Management, University of Santiago de Compostela,

[2]Soil Science and Agricultural Chemistry Department, University of Santiago de Compostela,

[3]Crop Production Department, University of Santiago de Compostela,

E-27002 Lugo, Spain

* Corresponding author. Tel.: (+34) 982 285900 Ext 23108; fax: (+34) 982 285926

E-mail address: cesar.cruzado@usc.es

Abstract:

This study proposes stand level models for estimating biomass yield, total energy and carbon sequestration in *Eucalyptus globulus* and *Eucalyptus nitens* plantations, on the basis of measurements made in 131 plots established at the usual range of initial forest densities for southwestern Europe. The timber volume, total aboveground biomass, logging residue biomass, crown biomass, carbon in aboveground biomass and soil organic layer, energy in aboveground biomass, energy in logging residue biomass and usable cellulose yield were represented in the form of isolines (taking mortality into account) and plotted against dominant height. These variables were calculated and compared with previously published data on two silvicultural options for short rotation forestry, one destined for bioenergy production and the other consisting of the standard silviculture regime applied to both species in southern Europe, considering the average site index for each species. Yield levels were higher in *Eucalyptus nitens* than in *Eucalyptus globulus* for all variables because of faster diameter increment at similar densities. The total yield in terms of biomass was 13.9-14.6 Mg ha^{-1} y^{-1} for *Eucalyptus globulus* and 20.4-21.5 Mg ha^{-1} y^{-1} for *Eucalyptus nitens*. Energy in aboveground biomass ranged between 233-245 GJ ha^{-1} y^{-1} for *Eucalyptus globulus* and 345-364 GJ ha^{-1} y^{-1} for *Eucalyptus nitens*, carbon accumulation rate in aboveground biomass and soil organic layer was 6.9-7.2 Mg ha^{-1} y^{-1} for *Eucalyptus globulus* and 12.7-13.5 Mg ha^{-1} y^{-1} for *Eucalyptus nitens*, and usable cellulose was 5.7-5.9 Mg ha^{-1} y^{-1} for *Eucalyptus globulus* and 9.0-10.1 Mg ha^{-1} y^{-1} for *Eucalyptus nitens*. It was found that 50% increments in the initial density result in only marginal increments in biomass and usable cellulose yields.

Keywords: short rotation forestry, eucalypts, woody crops, density management diagrams, bioenergy production, carbon sequestration.

1. Introduction

Short rotation woody crops (SRWC) (grown in short rotation forestry: SRF) are an important potential source of cellulosic biomass, which can be used as solid fuel in the form of wood chips, pellets or charcoal, transformed into ethanol via a cellulosic platform and/or used in pyrolysis to generate syngas and other products [1]. The establishment of single stem stands and subsequent replanting or coppicing is the most common management regime in SRF, and decisions about replanting and coppicing should consider: i) the yields from both options ii) establishment costs, and iii) desired dimensions of the final product [2].

The genus *Eucalyptus* has been used in forestation in Europe since the early 19th century because of its high productivity and plasticity. The total area currently occupied by *Eucalyptus* plantations in southern Europe is approximately 14000 km^2, with *Eucalyptus globulus* being the most common species but with an increasing proportion of *Eucalyptus nitens*, which is grown successfully as a frost-tolerant species. Both species belong to the subgenus *Symphyomyrtus*, known to produce larger average tree sizes and to be more productive than species of the subgenus *Monocalyptus* [3-5]. The management objective of these plantations in southern Europe is currently the production of wood pulp or fibreboard, although logging residues and the bark derived from the harvesting operations are increasingly used as biofuel to produce thermal energy and electricity.

The ideal characteristics of an energy crop are: i) high yield, ii) low energy input for production, iii) low cost, iv) minimal contents of contaminants and v) low nutrient requirements [6]. In this sense, *Eucalyptus* species adapt well to energy production, because of the higher yield and lower water and nutrient requirements than for poplars and willows [1]; *Eucalyptus* species accounted for 38% of total SRF plantations throughout the world in 2003 [7]. Before establishment of a plantation it is important to consider the desired combination of stem density and rotation. For species that must be established from seedlings, the application of narrow inter- and intra- row spacing would lead to very high costs and low ratios of wood/other biomass components, wood/bark or percentage of cellulose. Moreover, the average size of tree decreases as N increases [8] and larger logs are more dense. Nutrient depletion is also less likely for longer rotations, which also provide product flexibility [9,10]. Eucalypts in southern Europe established at initial densities of 1000 to 2400 stems per ha can therefore supply the bioenergy industry as the main plantation objective or through the use of logging residues for energetic purposes.

Forest plantations develop from a collection of individual, freely growing trees, through the onset of competition, to full site occupancy and self-thinning. Stand development is commonly displayed as a trajectory of increasing mean tree size with decreasing stand density [11]. Dynamic stand density management diagrams (SDMD) illustrate the relationships among yield, density and density-dependent mortality at all stages of stand development. Their use has been proven to be an effective method for the design, display and evaluation of alternative density management regimes in the field of even-aged forestry [12]. The adaptation of such management tools to the field of short rotation forestry for bioenergy production may assist in the assessment of energy yield potential, optimum stand management in terms of density and rotation in comparison with other potentially useful woody species.

Yield level indicators are considered the most important factors regarding the suitability of a tree species growing in SRF [13]. Statistic growth models based on a wide range of empirical data are increasingly used in research on SRF yields, rather than growth trials [14], because results from small plots may not be representative [14-16]. SDMD are based on relatively large plots established in commercial plantations and therefore provide more realistic yield estimations.

The objectives of the present study were to provide a management tool for estimating biomass and bioenergy production and carbon sequestration in *Eucalyptus globulus* and *Eucalyptus nitens* planted at the observed range of initial stockings in southern Europe, and to propose and compare two standard crop management regimes for both species.

2. Materials and methods

2.1. Source of data

For development of SDMD, a network of 131 unthinned plots was established in north-west Spain, 55 plots of *Eucalyptus globulus* and 76 of *Eucalyptus nitens*. The plots are located in a temperate Atlantic zone, with an average annual precipitation of 1100-1500 mm for both species and an average annual temperature of 13.9ºC and 13.2ºC, respectively. Average winter temperature is 10ºC for *Eucalyptus globulus* and 8.2ºC for *Eucalyptus nitens*. The coordinates of the plots were 43º41'80''- 42º52'00'' N and 8º24'11''- 7º03'56'' W (Figure 1).

The plots were measured once (in winter) between 2006 and 2010, thus covering a chronosequence in the range 0 to 25 years. Two types of plots were considered: circular plots of radius 10 m and square plots of 20x20 m, a size well above the threshold of 100 to 150 m^2 established for accurate biomass estimation [17]. The diameter at breast height (*d*, cm) and total height (h, m) were measured in all trees in each plot. Diameters were measured twice (measurements at right angles to each other) to the nearest 0.1 cm, with calipers, and the arithmetic mean value was calculated. Height was measured with Vertex IV to the nearest 10 cm. The stand variables calculated directly from these measurements were: quadratic mean diameter (dg, cm), average stand diameter ($\bar{d}$, cm), average stand height ($\bar{h}$, m) and tree density (N, stems ha^{-1}).

Dominant height (H_0, m) was determined per plot by use of a local height-diameter relationship and considering the 100 thickest stems per hectare [18]. Site index (SI, m) was calculated from local models [19,20], known to be valid for a single stem rotation in northern Spain. As the reference ages in these models are not the same (10 and 6 years for *Eucalyptus globulus* and *Eucalyptus nitens* respectively), the SI values cannot be directly compared. The volume of each tree was determined from taper functions [20,21]. The values were added to determine the stand volume (V, m^3 ha^{-1}).

2.2. Biomass and energy calculations

The total aerial biomass, logging residue biomass (branches and stem bark) and crown biomass (leaves and branches), were determined from single tree biomass equations developed in this study for *Eucalyptus nitens*, and fitted with data for *Eucalyptus globulus* [22], which are shown in Table 1. Both systems of equations were fitted simultaneously for samples of 36 *Eucalyptus globulus* trees and 40 *Eucalyptus nitens* trees respectively, by the seemingly unrelated regression method (*SUR*) and the MODEL procedure of SAS/ETS® [23].

The following biomass stand variables were calculated: total aerial biomass (W, Mg ha^{-1}), logging residue biomass (W_w, Mg ha^{-1}), considered as all the compartments except for stem and leaves and crown biomass (Wc, Mg ha^{-1}), in this case for all the compartments except stem, bark and dead branches under the crown. These values were calculated by summing the individual tree values corresponding to the compartments of interest.

The energy in aboveground biomass (E TJ ha^{-1}) and energy in logging residues (E_w TJ ha^{-1}) were determined by the low heating value (LHV, kJ kg^{-1}), calculated from expression (1) from the high heating value (HHV, kJ kg^{-1}) and the proportion of hydrogen in the dry matter (H_d, %) reported for both species [24-25]. The energy values were first determined at tree level as for the other variables.

$$LHV = HHV - \left(\frac{2442\,9H_d}{100}\right) \qquad (1)$$

The usable cellulose (UC, Mg ha^{-1}) was estimated from the volume under bark data for each plot and the average specific consumption of wood for pulp production, which is usually evaluated as inside bark wood volume (m^3) required to produce a dry weight of pulp, considering an average value of 3.2 m^3 Mg^{-1} for *Eucalyptus globulus*, and 3.8 m^3 Mg^{-1} for *Eucalyptus nitens* [26].

2.3. Carbon estimation

The concentrations of carbon in each biomass component were determined for the sample of trees used to derive biomass equations, by ignition in a LECO CNS-ICP 2000 element analyzer. Carbon in aboveground biomass was calculated from biomass equations and the carbon concentration at tree level (Table 1) was calculated by adding the values at plot level and expressing the values per hectare.

The carbon accumulated in soil organic layer was evaluated in only 40 plots per species by collecting 5 random samples per plot in square containers (30x30 cm) and determining the oven dry weight per unit surface area. The concentrations of carbon in litter were determined after ignition in a LECO CNS-ICP 2000 element analyzer, and average values of 46.94% and 47.68% were obtained for *Eucalyptus globulus* and *Eucalyptus nitens* respectively.

Total aboveground carbon (C Mg ha^{-1}) was then calculated for each plot as the sum of the total carbon in aboveground biomass and the carbon in the soil organic layer. Summary statistics, including the mean, maximum, minimum and standard deviation for each of the main stand variables calculated are shown in Table 2.

2.4. Development and construction of Stand Density Management Diagrams

The model developed in this paper for constructing SDMD includes a system of 9 equations, a density index and the mortality model as basic components. In the system of equations 2-10, N and H_0 are exogenous variables (defined independently of the system), V, W_w, W_c, C, E, E_w and UC are the endogenous variables (variables that the model is intended to explain or predict), and d_g is the endogenous instrumental variable [27]. The first equation (2) relates quadratic mean diameter to the number of stems per hectare and the dominant height. This equation is based on the relationship among average tree size, density and an indicator of productivity (i.e. [28,29]). The remaining equations (3-10) relate the stand yield (expressed in several ways), to quadratic mean diameter, number of stems per hectare and dominant height.

$$dg = b_0 \cdot N^{b_1} \cdot H_0^{b_2} \tag{2}$$

$$V = b_3 \cdot dg^{b_4} \cdot H_0^{b_5} \cdot N^{b_6} \tag{3}$$

$$W = b_7 \cdot dg^{b_8} \cdot H_0^{b_9} \cdot N^{b_{10}} \tag{4}$$

$$W_w = b_{11} \cdot dg^{b_{12}} \cdot H_0^{b_{13}} \cdot N^{b_{14}} \tag{5}$$

$$W_c = b_{15} \cdot dg^{b_{16}} \cdot H_0^{b_{17}} \cdot N^{b_{18}} \tag{6}$$

$$C = b_{19} \cdot dg^{b_{20}} \cdot H_0^{b_{21}} \cdot N^{b_{22}} \tag{7}$$

$$E = b_{23} \cdot dg^{b_{24}} \cdot H_0^{b_{25}} \cdot N^{b_{26}} \tag{8}$$

$$E_w = b_{27} \cdot dg^{b_{28}} \cdot H_0^{b_{29}} \cdot N^{b_{30}} \tag{9}$$

$$UC = b_{31} \cdot dg^{b_{32}} \cdot H_0^{b_{33}} \cdot N^{b_{34}} \quad (10)$$

Because of the existence of correlation between error components of the independent variables and dependent variables, the full information maximum likelihood method (*FIML*) was applied in the fitting process. The system of equations was fitted simultaneously by use of the MODEL procedure of the SAS/ETS® system [23]. In the absence of convergence, equations were fitted by subgroups. The adjusted coefficient of determination and the root mean square error were used to check the accuracy of the models.

Mortality models were also considered for evaluating the non density dependent mortality. The models used for *Eucalyptus globulus* [30] and *Eucalyptus nitens* [31] are shown as equations (11 and 12 respectively).

$$N_1 = N_0 \cdot e^{-0,0281 \cdot (t_1 - t_0)} \quad (11)$$

$$N_1 = N_0 - N_0 \cdot \left(1 - e^{\left(-e^{A}\right)}\right), \text{ with } A = -8.6 + 0.1124 \cdot S + 0.1487 \cdot \left(\frac{t_0 + t_1}{2}\right) - 0.0067 \cdot \left(\frac{t_0 + t_1}{2}\right)^2 \quad (12)$$

where N_0 and N_1 are the number of stems per hectare at the age of t_0 and t_1 years respectively, and S (site index, m) is the dominant height at the age 15 years, estimated by the Candy model.

The SDMD were constructed by representing dominant height on the X-axis and the number of stems per hectare in logarithmic scale on the Y-axis. The quadratic mean diameter isolines were represented in the diagrams taking constant values for dg and solving for N the equation (2). The isolines for the equations (3-10) were represented in the diagrams solving dg in each equation with (2), assuming constant values for each variable and solving for N. Mortality isolines were also represented for each species. Since conversion between t and H_0 depends on site quality conditions, average observed SI values for each species were considered (Table 2).

Two SDMD were represented per species, one for carbon sequestration estimation (including additional isolines for quadratic mean diameter, carbon in aboveground biomass and organic soil, Hart-Becking index, mortality and sample plots for each species), and another for bioenergetic yield estimation (including additional isolines for usable cellulose, aboveground biomass energy, harvest limits and mortality).

2.5. Assessment of density limits and harvest limits

The relative spacing index (*HI*, %) was used to characterize the competence level at each development stage [32], this was calculated as the ratio between the average distance among trees and the dominant height expressed as a percentage, with expression (13) and considering square spacing [33-35].

$$RS = \frac{10000}{H\sqrt{N}} \tag{13}$$

In order to determine the threshold density due to the self-thinning effect or full density curve FDC [36], the -3/2 power law was used [37], considering the average crown biomass $\overline{W_c}$ [38] as an indicator of crowding. This is because the stem occupies a negligible space with respect to the crown and roots, and therefore crowding is more closely related to crown biomass than to total aerial biomass.

$$\overline{W_c} \cdot N^{3/2} = K \tag{14}$$

As a convention, $\overline{W_c}$ at 1000 stems ha^{-1} (W_{x1000}) has been considered for defining the FDC [39,40], thus enabling determination of the value of the constant *K* that defines the curve. In this study, the average crown biomass (kg tree^{-1}) was plotted against stand density to determine the maximum average crown biomass at 1000 stems ha^{-1} (W_{c1000}, kg tree^{-1}). The FDC equation was then derived from (14) by substituting *K* for $W_{c1000} 1000^{3/2}$.

Although the -3/2 power law of self-thinning. [37] is assumed to be valid for all species and locations, some factors such as severe nutrient deficiencies [41,42], climatic conditions and artificial shading [43] may affect the trajectory of FDC. This implies that it is more appropriate to define a full density zone (FDZ), in which the probability of mortality due to the self-thinning effect is very high [36]. The lowest boundary limit of FDZ was determined as 70% of W_{c1000} [44]. Both limits of FDZ were represented in the diagrams by solving equation (14) for N.

Mechanized harvesting implies a size limitation due to the machinery used. Isolines of 10 and 20 cm of average stump diameter ($\bar{d}_{st}$, cm) were therefore represented in the diagrams. For this, a linear relationship between dg and $\bar{d}$ was fitted for both species. $\bar{d}_{st}$ can be estimated accurately from the average diameter at breast height by use of a linear model [45]. An already published regional model was used to estimate *Eucalyptus globulus* $\bar{d}_{st}$ [21], and a similar model, developed with data collected in the plots established in the present study, was used to estimate *Eucalyptus nitens* $\bar{d}_{st}$.

3. Results

3.1. Model parameters and additional relations

Results of the non-linear fit of equations 2-10, the coefficient estimates and the regression statistic values are shown in Table 3. All coefficients were significant at $P<0.05$, and the models accounted for more than 84% of the total variability in the quadratic mean diameter, and more than 94% of the total variability in productivity equations (3-10).

As expected, the least accurate models were those predicting dg, since the approach used in developing this type of diagram is to predict yield rather than increment, which makes them of little use, relative to dynamic growth models, for simulating a broad range of silvicultural regimes [46]. With regard to the productivity equations, the C model was the least accurate, because the carbon in the soil organic layer is barely related to the independent variables considered, and is more closely related to time since last perturbation. The changes in total carbon in the aboveground biomass and in the soil organic layer over time are shown in Figure 2.

The dynamics of accumulation were quite different in both compartments (Fig.2), while there was a high rate of accumulation of aboveground biomass carbon in both species (although dependent of site quality, Carbon at 8.3 Mg ha^{-1} y^{-1} on average), the carbon in the litter tended to stabilize at 5-7 years in both species, and reached values of Carbon at 20 and 30 Mg ha^{-1} at this age in *Eucalyptus globulus* and *Eucalyptus nitens* plantations.

The relation between the average crown biomass (kg tree^{-1}) and the number of stems per hectare for each plot and species, including several isolines of W_{c1000}, are shown in Figure 3. If we consider only the plots with low *IH* values and that probably undergo self-thinning [47], the most reasonable values for the W_{c1000} are 60 kg tree^{-1} for *Eucalyptus globulus* and 50 kg tree^{-1} for *Eucalyptus nitens*. This indicates that *Eucalyptus nitens* tolerates lower densities than *Eucalyptus globulus*, which is consistent with previous findings for this species [5,13]. These values are equivalent to aboveground biomass of 360 kg tree^{-1} for *Eucalyptus globulus* and 285 kg tree^{-1} for *Eucalyptus nitens*, values similar to the self-thinning threshold defined to parameterize the 3PG model for *Eucalyptus globulus* in Australia (300 kg tree^{-1}, [39]).

The parameter values for the linear models of $\bar{d}$ estimation from *dg* for each species are shown in Table 4. The model accuracy was very high for both species, allowing the incorporation of the harvesting limits for $\bar{d}_{st}$ of 10 and 20 cm.

3.2. Stand density management diagrams

The SDMD obtained for *Eucalyptus globulus* and *Eucalyptus nitens* are shown in Figures 4-7. The isolines for quadratic mean diameter, carbon in biomass and organic soil, Hart-Becking index and mortality, as well as the positions of the sample plots are shown in Figures 4 and 6. The isolines for usable cellulose, aboveground biomass energy, harvest limits and mortality are shown in Figures 5 and 7. Although SDMD provide useful graphic information about stand development stages, for more accurate estimation, equations 2-10 and the parameters shown in Table 3 must be used.

As can be seen in the SDMD, *dg* decreases for a given H_0 as N increases because of increased competition for resources, which results in a smaller average tree size [18,48-50]. The pattern of *dg* isolines is parallel to that observed for the harvest limits, and thus a threshold established for basal diameter would mean that a combination of initial planting density and dominant height at harvest would have to be considered.

For comparable stages of stand development (in terms of H_0 and N), *Eucalyptus nitens* accumulates more carbon in biomass and soil organic layer, and this effect is partly attributable to the higher rate of accumulation of C in soil organic layer (Figures 4 and 6).

The shape of biomass-related isolines (W, W_w, W_c, E and E_w) are more vertical than the volume-related isolines (V and UC) (Figures 5 and 7). This indicates that biomass-related isolines are less sensitive to changes in N than volume-related isolines. Moreover, for comparable stages of stand development, *Eucalyptus nitens* has more energy in aboveground biomass and usable cellulose than *Eucalyptus globulus*, because of faster diameter growth at comparable levels of N and H_0. These results are consistent with those of other studies for single stem crops of *Eucalyptus nitens* at 2200 stems ha^{-1} [5].

The changes in live-tree densities are shown in all the diagrams and allow estimation of expected natural mortality after planting in a scenario of no thinning, which is generally applied to woody crops destined for energy or fibre production. It must be considered that these trends were calculated by considering the average site index for both species and thus a site specific calculation using equations (11) and (12) is recommended if greater accuracy is sought. A high plantation density, together with longer rotations, results in high self-thinning mortality and unstable stems, as already corroborated [13]. As the initial density increases, the boundary of the FDZ is closer in terms of H_0 and therefore the management window is smaller. Although the relationship between the number of stems per hectare and the average tree size is a good indicator of density and therefore of competence, there are other factors that affect the self-thinning process, such as tree distribution and accumulation of gaps [51], which is not important when a regular square distribution is considered, but could be in the case of paired row layouts.

In the SDMD proposed here, several harvesting limits were represented. The $\bar{d}_{st}$ 10 cm limit defines the area in which a chip harvester may be more profitable. The $\bar{d}_{st}$ 10 and 20 cm limits define the area where a multi-cutter harvester may be more cost effective, whereas average basal diameters above $\bar{d}_{st}$ 20 cm would limit the choice to traditional single-stem harvesters.

Since all models depend on *N*, the production costs can be easily determined, and together with a correct estimate of site quality, will determine the time needed to obtain the desired products and therefore the economic profitability of the plantation.

3.3. Practical example of SDMD for determining energy production

SDMD can be used to estimate production from a given stand development stage (*N* and H_0), or to estimate the minimum density that can provide a certain output for an average tree size. As a practical example, two silvicultural alternatives were simulated for each species, with initial densities of 2400 and 1600 stems ha^{-1}, representative of an energy option and a standard southern European pulp production target, respectively. The rotation time (*T*) was defined as the time that allows efficient harvesting of the crop by a multi-cutter harvester ($\bar{d}_{st}$ 20 cm) in the case of the energy target for an average site index. For the standard pulp silviculture, stand growth was simulated until one of the two species reached the FDZ area, which for *Eucalyptus nitens* occurred at a dominant height of 29 m. The stand development stages at the time of harvest and rotation time for the average site index are shown for both alternatives and species (Table 5). The predicted *dg* at the end of rotation and yield values for V, W, W_w, W_c, C, E, E_w and *UC* for the two silvicultural alternatives are also shown.

The total aboveground biomass yield for all fractions ranged between 13.9-14.6 Mg ha^{-1} y^{-1} for *Eucalyptus globulus* and between 20.4-21.5 Mg ha^{-1} y^{-1} for *Eucalyptus nitens* (Table 5). The mean annual increment in terms of biomass was only marginally higher for the high density silviculture, although the rotation age was also shorter in this case. The values for the expected yield in terms of energy or usable cellulose were higher for *Eucalyptus nitens*, although direct comparison is difficult, as the species grow in different areas.

4. Discussion

4.1. Model performance and limitations

The model presented here represents a system of related equations that enable accurate estimation of crop yield in terms of oven dry biomass, total energy, usable cellulose and other variables, and thus provides a powerful tool for decision making as regards woody crops of the species studied. The diagrams show the crop development as dominant height increases, and are therefore independent of age and valid for applying to different breeding materials and sites for each species, provided the change in dominant height with age is known in each case. These empirical statistically-based tools can also be combined with process-based models if the detailed information required in this case is available.

Woody biomass can be converted via combustion, gasification, pyrolysis and fermentation, and the energy recovered depends on the conversion technology [6]. Although the energy obtained from *LHV* is a theoretical value that can only be achieved at 0% moisture, the information obtained from the diagrams, particularly the share of logging residues, and the proportion of cellulose or stem volume, is useful for determining the suitability of the biomass produced for subsequent processing.

The models provided here are only valid for single stem rotations, which is an important constraint to be considered. However, this is not a key limitation in the case of *Eucalyptus nitens*, because some studies have shown the poor coppicing ability of *Eucalyptus nitens* [13,52], at least for the breeding materials currently in use. Changes in growth patterns and relationships among stand variables after coppicing have been shown, particularly the change in basal area derived from the sprout number per stool [16]. It is therefore necessary to obtain a similar model for *Eucalyptus globulus* coppice stands in order to assess the long term productivity.

One of the main advantages of the models provided in this paper is the possibility of assessing the economic profitability of SRC with eucalypts, because many variables are needed to calculate the cash flow throughout the rotation. Most production costs, from establishment to delivery, can be calculated as they are density-dependent, as is the case of plantation, localized fertilization and weed control. Plant material may account for up to 65% of establishment costs and any advantage gained by high planting rates may be outweighed by increasing costs [15]. Stand harvesting costs constitute a major portion of total production costs, and may have effects as important as those of stand establishment costs [53]. Harvest operations represent up to 70% of the cost in the overall supply chain, and therefore less frequent harvesting reduces the cost of biomass production per unit [15]. Moreover, average tree size is the most important factor in harvesting costs [53]. The information provided in the diagrams, particularly the average basal diameter, is also essential for deciding what type of harvesting to carry out, i.e. whole stem harvesting or chip harvesting.

4.2. Carbon sequestration

The diagrams obtained in this paper and the fitted equations constitute a powerful tool for assessing carbon sequestration in eucalypts grown in SRF. The isolines plotted in the diagrams range between 20 and 200 Mg ha^{-1} for carbon in aboveground biomass and litter.

Since no information was obtained for root biomass it was not possible to assess sequestration in this compartment, which is an important consideration because root biomass is usually left in situ after the crop is harvested.

The values for carbon in litter show greater accumulation of C in the litter resulting from *Eucalyptus nitens* than in *Eucalyptus globulus* crops. Net production in a forest should be assessed as the sum of biomass accumulation and annual litter production, which in *Eucalyptus globulus* plantations of density 4167 stems ha^{-1} may reach 13.4 Mg ha^{-1} y^{-1}, and as much as 10-20% of the total biomass production at age 3 years [54]. Although this litter can hardly be used for energy production, estimation of the quantity is important for estimating carbon accumulation and nutrient cycle return. Although the soil mineral layer was not considered here, carbon accumulation in this pool is very important because the lifespan of the carbon is longer than in biomass and in the soil organic layer [55].

4.3. Comparison of data from other studies

The biomass yields (Table 5) are higher than the 1-9 Mg ha^{-1} y^{-1} reported for 4-year-old *Eucalyptus globulus* planted at a density of 2196 stems ha^{-1} [56], but lower than the 24 Mg ha^{-1} y^{-1} observed in 3-year-old plantations of the same species in New Zealand, established at a density of 4167 stems ha^{-1} and irrigated with effluent. Non irrigated stands yielded as much as 19.3 Mg ha^{-1} y^{-1} [10]. *Eucalyptus globulus* planted at densities of 20,000, 30,000 and 40,000 stems ha^{-1} in Portugal [57] yielded 16, 21 and 19 Mg ha^{-1} y^{-1} after 2 years. The general effect is therefore a similar average yield (obtained early on because of the initial high stocking density) but with a decrease in the average tree size [14]. Referenced yield data for *Eucalyptus nitens* in SRF are scarce and values are very low compared with those observed in the present study. In New Zealand, yield values of 3-7.3 Mg ha^{-1} y^{-1} have been reported for single stems established at a density of 5000 stems ha^{-1} and first coppice rotation, respectively, with very low survival [13]. As regards other *Eucalyptus* species, a study collecting yield data for several *Eucalyptus* species in Australia reported values of between 11 and 16 Mg ha^{-1} y^{-1} [58]. Another study in the USA reported *Eucalyptus* yields as high as 40 Mg ha^{-1} y^{-1} for a wide range of sites [59]. The average yields for *Eucalyptus* species in a single stem rotation at a density of 2200 stems ha^{-1} reported for a species-comparative study in New Zealand ranged between 9.6 and 15.5 Mg ha^{-1} y^{-1} [5], which are the highest reported values for the species, with high survival rates and larger average tree size. The values observed here were similar or higher and were determined from commercial sized plots with conservative assumptions for site quality.

With regard to energy production at the end of rotation, the predicted values ranged between 3.4-3.5 and 4.0-4.1 TJ ha^{-1} for *Eucalyptus globulus* and *Eucalyptus nitens* respectively, well above the values reported for poplar (173-259 GJ ha^{-1}; 10-15 Mg ha^{-1} y^{-1}) and willow (187-280 GJ ha^{-1}; 10-15 Mg ha^{-1} y^{-1}) grown as short rotation woody crops. Mean values ranged from 245 to 345 GJ ha^{-1} y^{-1}, still far from the average range for eucalypt plantations in Aracruz (450 to 650 GJ ha^{-1} y^{-1}, [60]). The annual logging residue energy yield was 33-35 and 53-54 GJ ha^{-1} y^{-1} for *Eucalyptus globulus* and *Eucalyptus nitens* respectively, similar to the 65 GJ ha^{-1} y^{-1} estimated for both species together, also in northern Spain [25].

Rotations simulated for the bioenergy alternative in this paper are longer than the average considered in SRC, but there are positive effects of this practice. If wood is the main biomass compartment desired, longer rotations provide higher wood:bark ratios, as shown in Figure 8 for the data used in the present study. The wood:bark ratio can reach up to 80% in *Eucalyptus globulus* at 10 years [10], but data reported for *Eucalyptus nitens* at 3 years indicate a rather low value of 45% [5]. Moreover, longer rotations result in larger average tree size, and therefore harvest machinery is better able to discriminate between leaves and other tree fractions, which reduces the nutrient exports and ash production. Bark and leaves contain the highest amounts of ash in all aboveground biomass compartments, with reported values of

1.5-2 times [25], and even 10 times [61] the wood ash content; this is an important problem if combustion is the chosen methods of biomass transformation, as the high ash content can damage the boilers used. Longer rotations are also a good option if the goal is product flexibility [14]. The results of the present study for the single stem rotation showed that 50% increments in initial density result in only marginal increases in yield as well as decreases in rotation, as previously observed [53].

4. Conclusions

Management tools for estimation of bioenergy production and carbon sequestration in single stem *Eucalyptus* plantations are presented in the form of dynamic SDMD. These models allow yield simulations for a range of initial density and rotation age options and provide information about the value of the crops, by use of input data usually available from routine forest inventories. The observed yields for *Eucalyptus globulus* and *Eucalyptus nitens* planted at densities of 1600-2400 stems ha^{-1} in single stem rotation are similar to those observed for the higher densities usually used in SRF. *Eucalyptus nitens* displayed faster diameter growth than *Eucalyptus globulus* planted at similar densities. Mean values of potential annual energy production from total biomass, except leaves, for average site indices for both species in northern Spain ranged between 233-245 and 345-364 GJ ha^{-1} y^{-1} for *Eucalyptus globulus* and *Eucalyptus nitens*, respectively. The options simulated in this paper display good product flexibility and would provide high wood: bark ratios.

Acknowledgements

The authors thank Pablo Mansilla and Nohelia Díaz for assisting with fieldwork. The study was funded by the Spanish Ministry of Education and Science (SUM2006-00006-00-00, AGL2010-22308-CO2-01/FOR) and a FPU-MEC Spanish Fellowship awarded to the correspondent author.

References

[1] Johnson J, Coleman MUFS, Gesch R, Jaradat A, Mitchell R, Reicosky D, et al. Biomass-bioenergy crops in the United States: A changing paradigm. Amer J Plant Sci Biotech 2007;1(1):1-28.

[2] Rockwood DL, Carter DR, Langholtz MH, Stricker JA. *Eucalyptus* and *Populus* short rotation woody crops for phosphate mined lands in Florida USA. Biomass Bioenerg 2006;30(8-9):728-34.

[3] Davidson NJ, Reid JB. Comparison of the early growth characteristics of the *Eucalyptus* subgenera *Monocalyptus* and *Symphyomyrtus*. Aust J Bot 1980;28:453-61.

[4] Turnbull CRA, McLeod DE, Beadle CL, Ratkowsky DA, Mummery DC, Bird T. Comparative early growth of *Eucalyptus* species of the subgenera *Monocalyptus* and *Symphyomyrtus* in intensively-managed plantations in southern Tasmania. Aust For 1993;56(3):276-86.

[5] Sims REH, Senelwa K, Maiava T, Bullock BT. *Eucalyptus* species for biomass energy in New Zealand—I: Growth screening trials at first harvest. Biomass Bioenerg 1999;16(3):199-5.

[6] McKendry P. Energy production from biomass (part 1): overview of biomass. Bioresour Technol 2002;83(1):37-46.

[7] FAO. State of World' Forests. Rome: Food and Agriculural Organization of the United Nations; 2003.

[8] Bullard MJ, Mustill SJ, Carver P, Nixon PMI. Yield improvements through modification of planting density and harvest frequency in short rotation coppice *Salix* spp.-2. Resource capture and use in two morphologically diverse varieties. Biomass Bioenerg 2002;22(1):27-39.

[9] Ericsson T. Nutrient dynamics and requirements of forest crops. N Z J For Sci 1994;24(2-3):133-68.

[10] Guo LB, Sims REH, Horne DJ. Biomass production and nutrient cycling in *Eucalyptus* short rotation energy forests in New Zealand. I: biomass and nutrient accumulation. Bioresour Technol 2002;85(3):273-83.

[11] Long JN, Dean TJ, Roberts SD. Linkages between silviculture and ecology: examination of several important conceptual models. For Ecol Manag 2004;200(1-3):249-61.

[12] Newton P. Stand density management diagrams: Review of their development and utility in stand-level management planning. For Ecol Manag 1997;98(3):251-65.

[13] Sims REH, Maiava TG, Bullock BT. Short rotation coppice tree species selection for woody biomass production in New Zealand. Biomass Bioenerg 2001;20(5):329-35.

[14] Dickmann DI. Silviculture and biology of short-rotation woody crops in temperate regions: Then and now. Biomass Bioenerg 2006;30(8-9):696-5.

[15] Mitchell CP, Stevens EA, Watters MP. Short-rotation forestry- operations, productivity and costs based on experience gained in the UK. For Ecol Manag 1999;121:123-36.

[16] Sims REH, Senelwa K, Maiava T, Bullock BT. *Eucalyptus* species for biomass energy in New Zealand-Part II: Coppice performance. Biomass Bioenerg 1999;17(4):333-43.

[17] Specht A, West PW. Estimation of biomass and sequestered carbon on farm forest plantations in northern New South Wales, Australia. Biomass Bioenerg 2003;25(4):363-79.

[18] Assmann E. The principles of forest yield study. Oxford: Pergamon Press; 1970.

[19] Fernández López AB. Evaluación de la producción y productividad del monte bajo de *Eucalyptus globulus*. Centro de Investigaciones Forestales de Lourizán, Pontevedra: Consellería de Agricultura, Gandería e Montes; 1982. 69 p.

[20] Pérez-Cruzado C. Herramientas de gestión para plantaciones de *Eucalyptus nitens* (Deane & Maiden) Maiden con el objetivo de fijación de carbono. Lugo: University of Santiago de Compostela; 2009. 77 p.

[21] Sánchez F, Ucha P, Rojo, A. Stem taper functions and volume equations with product classification for *Eucalyptus globulus* Labill. in Galicia (NW Spain). In: Alvarez JG, Goulding C, Rojo A, Rodríguez-Soalleiro R, Zoralioglu T, Ruiz Gonzalez AD. International IUFRO 4.04.06 Meeting. The Economics and Management of High Productivity Plantations; 27-30 September 2004; Lugo; University of Santiago de Compostela; 2004. p. 1-21.

[22] Brañas J, González-Río F, Rodríguez Soalleiro R, Merino A. Biomasa maderable y no maderable en plantaciones de eucalipto. Cuantificación y estimación. CIS-Madera 2000;4:72-5.

[23] SAS Institute Inc. SAS/STAT 9.1 User's Guide. Cary, N.C.; 2004.

[24] Pérez S, Renedo CJ, Ortiz A, Mañana M, Silió D. Energy evaluation of the *Eucalyptus globulus* and the *Eucalyptus nitens* in the north of Spain (Cantabria). Thermochim Acta 2006;451(1-2):57-64.

[25] Pérez S, Renedo CJ, Ortiz A, Manana M. Energy potential of waste from 10 forest species in the North of Spain (Cantabria). Bioresour Technol 2008;99(14):6339-45.

[26] Cotterill P, Macrae S. Improving *eucalyptus* pulp and paper quality using genetic selection and good organization. Tappi J 1997;80(6):82-9.

[27] Borders BE. Systems of equations in forest stand modeling. For Sci 1989;35(2):548-56.

[28] C. J. Goulding. Simulation technique for a stochastic model of growth of Duglas-fir. Vancouver, British Columbia: University of British Columbia; 1972.

[29] Long JN, Shaw JD. A density management diagram for even-aged ponderosa pine stands. W J A F 2005;20(4):205-15.

[30] García O, Ruiz F. A growth model for eucalypt in Galicia, Spain. For Ecol Manag 2003;173(1-3):49-62.

[31] Candy SG. Growth and yield models for *Eucalyptus nitens* plantations in Tasmania and New Zealand. Tasforests 1997;9:167-94.

[32] Gadow K, Hui G. Modelling forest development. Dordrecht: Kluwer Academic Publishers; 1999.

[33] Barrio Anta M, Álvarez González JG. Development of stand density management diagram for even aged pedunculate oak stand and its use in designing thining schedules. Forestry 2005;78(3):209-16.

[34] Barrio-Anta M, Balboa-Murias MA, Castedo-Dorado F, Diéguez-Aranda U, Álvarez-González JG. An ecorregional model for estimating volumen, biomass and carbon pools in maritime pine stands in Galicia (Northwestern Spain). For Ecol Manag 2006;223:24-34.

[35] Castedo-Dorado F, Crecente-Campo F, Álvarez-Álvarez P, Barrio-Anta M. Development of a stand density management diagram for radiate pine stands including assessment and stability. Forestry 2009;82(1):1-15.

[36] Jack SB, Long JN. Linkages between silviculture and ecology: an analysis of density management diagrams. For Ecol Manag 1996;86(1-3):205-20.

[37] Yoda K, Kira T, Ogawa H, Hozumi K. Self-thinning in overcrowded pure stands under cultivated and natural conditions. J Inst Polytech, Osaka City Univ, Ser D 1963;14:107-29.

[38] Zeide B. How to measure stand density. Trees-Structure and Function 2005;19(1):1-14.

[39] Sands PJ, Landsberg JJ. Parameterisation of 3-PG for plantation grown *Eucalyptus globulus*. For Ecol Manag 2002;163(1-3):273-92.

[40] Almeida AC, Landsberg JJ, Sands PJ. Parameterisation of 3-PG model for fast-growing *Eucalyptus grandis* plantations. For Ecol Manag 2004;193(1-2):179-95.

[41] Lonsdale WM, Watkinson AR. Light and self-thinning. New Phytol 1982;90(3):431-45.

[42] Morris EC, Myerscough PJ. Self-thinning and competition intensity over a gradient of nutrient availability. J Ecol 1991;79(4):903-23.
[43] Aikman DP, Watkinson AR. A model for growth and self-thinning in even-aged monocultures of plants. Ann Bot 1980;45(4):419-27.
[44] DeBell DS, Whitesell CD. Diameter-density relationships provide tentative spacing guidelines for *Eucalyptus saligna* in Hawaii. Pacific Southwest Forest and Range Experiment Station: Forest Service U.S. Department of Agriculture; 1988. 3 p. Res Note PSW-397.
[45] Diéguez-Aranda U, Barrio Anta M, Castedo Dorado F, Balboa Murias M. Estimación del diámetro normal y del volumen del tronco a partir de las dimensiones del tocón para seis especies forestales comerciales de Galicia. Invest Agrar Sist Recur For 2003;12(2):131-9.
[46] García O. The state-space approach in growth modelling. Can J For Res 1994;24(9):1894-3.
[47] Lonsdale WM. The self-thinning rule: dead or alive? Ecology 1990;71(4):1373-88.
[48] Hamilton GJ. The dependence of volume increment of individual trees on dominance, crown dimensions, and competition. Forestry 1969;42(2):133-44.
[49] Curtis RO. Stand density measures: an interpretation. For Sci 1970;16(4):403-14.
[50] Dean TJ, Long JN. Influence of leaf area and canopy structure on size−density relations in even-aged lodgepole pine stands. For Ecol Manag 1992;49(1-2):109-17.
[51] Li BL, Wu H, Zou G. Self-thinning rule: a causal interpretation from ecological field theory. Ecol Modell 2000;132(1-2):167-73.
[52] Little KM, Gardner RAW. Coppicing ability of 20 *Eucalyptus* species grown at two high-altitude sites in South Africa. Can J For Res 2003;33(2):181-9.
[53] Whitesell CD, DeBell DS, Schubert TH, Strand RF, Crabb TB. Short-rotation management of *Eucalyptus*: guidelines for plantations in Hawaii. Pacific Southwest Forest and Range Experiment Station: Forest Service U.S. Department of Agriculture; 1992. 30 p. Tech Rep PSW-GTR-137.
[54] Toky OP, Ramakrishnan PS. Secondary succession following slash and burn agriculture in north-eastern India: I. Biomass, litterfall and productivity. J Ecol 1983;71:735-45.
[55] Romanya J, Cortina J, Falloon P, Coleman K, Smith P. Modelling changes in soil organic matter after planting fast-growing *Pinus radiata* on Mediterranean agricultural soils. Eur J Soil Sci 2000;51(4):627-41.
[56] Cromer RN, Raupach M, Clarke ARP, Cameron JN. *Eucalypt* plantations in Australia- the potential for intensive production and utilization. Appita J 1975;29(3):165-73.
[57] Pereira JS, Madeira MV, Linder S, Ericsson T, Tomé M, Araújo MC. Biomass production with optimised nutrition in *Eucalyptus globulus* plantations. In: Pereira JS, editor. *Eucalyptus* for biomass productionBrussells: Commission of the European Communities; 1994, p. 13-30.
[58] Wise PK, Pitman MG. Nutrient removal and replacement associated with short-rotation eucalypt plantations. Aust For 1981;44(3):142-52.
[59] Yields of short rotation *Eucalyptus grandis* in high density plantings. Energy from biomass and wastes IV; January 21-25; Florida: Institute of Gas Technology; 1980.
[60] Moreira JXCR. Global biomass energy potential. Mitigation Adapt.Strat.Global Change 2006;11(2):313-33.
[61] Ragland KW, Aerts AJ. Properties of wood for combustion analysis. Bioresour Technol 1991;37(2):161-8.

TABLES

Table 1. Biomass equations for *Eucalyptus globulus* and *Eucalyptus nitens* in north-west Spain.

Species	Fraction	R^2*Adjust.*	*REMC* (kg)	*CC* (%)
Eucalyptus globulus	$w_w + w_{lb} = 0.01308 \cdot d^{1,870} \cdot h^{1,172}$	0.989	13.4	45.2
	$w_b = 0.01010 \cdot d^{2,484}$	0.932	3.82	42.5
	$w_{mb} + w_{sb} = 0.003685 \cdot d^{2,654}$	0.841	5.16	45.3
	$w_t = 0.01258 \cdot d^{1,705}$	0.586	0.971	46.4
	$w_l = 0.02949 \cdot d^{1,917}$	0.706	4.38	52.0
Eucalyptus nitens	$w_w + w_{lb} = 0.009400 \cdot d^{2,033} \cdot h^{1,056}$	0.990	17.9	50.1
	$w_b = 0.01342 \cdot d^{2,361}$	0.710	15.3	46.9
	$w_{mb} = 0.00005900 \cdot d^{3,760}$	0.897	6.01	49,8
	$w_{sb} = 0.01280 \cdot d^{1,858}$	0.756	2.24	49.8
	$w_t = 0.0009220 \cdot d^{2,632}$	0.831	2.09	51.5
	$w_l = 0.005300 \cdot d^{2,393}$	0.813	5.59	57.2
	$w_{db} = 0.1451 \cdot d^{1,403}$	0.397	10.6	50.4

where w_w is the wood biomass (up to 7 cm diameter over bark), w_b is the bark biomass in the stem, w_{lb} is the biomass of large branches (up to 7 cm diameter over bark), w_{mb} is the biomass of medium sized branches (diameters over bark between 7 and 2 cm), w_{sb} is the biomass of small branches (diameters over bark between 2 and 0,5 cm), w_t is the twig biomass (diameters over bark smaller than 0.5 cm), w_l is the leaf biomass, and w_{db} is the biomass of dead branches in the bottom stem (a large fraction of the weight in *Eucalyptus nitens*). The carbon concentrations for *Eucalyptus globulus* were obtained from a local study [22].

Table 2. Statistics for the main variables measured in the sample plots.

Variable	***Eucalyptus globulus***				***Eucalyptus nitens***			
	Mean	**Min.**	**Max.**	**S.D.**	**Mean**	**Min.**	**Max.**	**S.D.**
dg (cm)	16.32	1.291	36.44	8.01	19.60	6.452	35.23	5.39
G (m^2 ha^{-1})	27.80	0.092	81.98	20.00	35.33	2.185	81.98	16.92
$\bar{d}$ (cm)	15.29	1.200	35.64	7.67	18.66	6.248	34.06	5.20
$\bar{h}$ (m)	17.35	1,.268	32.07	7.92	19,.61	5.857	32.07	5.23
N (stems ha^{-1})	1182	446	1825	318	1152	446	2196	387
Ho (m)	22.86	1.10	40.50	10.44	24.54	7.40	40.41	7.08
SI (m)	23.33	8.99	36.32	6.47	16.30	8.80	26.20	4.90
V (m^3 ha^{-1})	291.18	0.064	1139.90	252.50	365.82	8.133	1129.46	223.86
W (Mg ha^{-1})	171.92	0.084	709.12	153.15	187.09	4.763	653.50	119.40
W_w (Mg ha^{-1})	28.88	0.033	110.51	24.77	43.87	2.456	132.30	24.08
W_c (Mg ha^{-1})	20.34	0.052	70.32	16.13	22.93	0.727	85.57	14.82
C (Mg ha^{-1})	101.12	0.040	325.84	74.17	106.92	26.608	358.51	65,.11
E (TJ ha^{-1})	2.88	0.001	11.93	2.58	3.20	0.081	11.17	2.04
E_w (TJ ha^{-1})	0,.45	0.001	1.74	0.39	0.71	0.040	2.14	0.39
UC (Mg ha^{-1})	71.62	0.009	305.55	65.46	82.80	1.678	262.29	51.72

Table 3. Non-linear regression coefficients and statistics obtained from simultaneous fitting of the system of 10 equations predicting quadratic mean diameter (*dg*, cm), stand volume (*V*, m^3 ha^{-1}), total aerial biomass (*W*, Mg ha^{-1}), crown biomass (W_c, Mg ha^{-1}), total carbon in aboveground biomass and soil organic layer (*C*, Mg ha^{-1}), logging residue biomass (W_w, Mg ha^{-1}), total aerial energy without leaves (*E*, TJ ha^{-1}), logging residue energy (E_w, TJ ha^{-1}), usable cellulose production (*UC*, Mg ha^{-1}).

Eucalyptus globulus

Equation	**Parameter estimates**				***Adjusted R^2***	***RMSE***
(2)	b_0=16.37744 (9.7711)	b_1=-0.38706 (0.0699)	b_2=0,.868226 (0.0858)		0.8480	3.1225
(3)	b_3=0.000064 (0.000018)	b_4=2.047556 (0.0504)	b_5=0.756605 (0.0482)	b_6=0.981972 (0.0235)	0.9950	17.8455
(4)	b_7= 0.000034 (5.775E-6)	b_8=2.132935 (0.0164)	b_9=0.732106 (0.0175)	b_{10}=0.97052 (0.0133)	0.9984	6.0913
(5)	b_{11}=0.000012 (1.79E-6)	b_{12}=2.457291 (0.0145)	b_{13}=0.077533 (0.0148)	b_{14}=1.036985 (0.0134)	0.9987	0.8934
(6)	b_{15}=0,.000021 (2.023E-6)	b_{16}=2.259985 (0.00986)	b_{17}=0.03626 (0.0109)	b_{18}=1.014372 (0.00884)	0.9992	0.4474
(7)	b_{19}=0.000073 (0.000029)	b_{20}=2.058496 (0.0528)	b_{21}=0.512052 (0.0602)	b_{22}=0.899273 (0.0426)	0.9911	6.9936
(8)	b_{23}=5.544E-7 (9.644E-8)	b_{24}=2.130056 (0.0168)	b_{25}=0.745888 (0.0179)	b_{26}=0.969512 (0.0136)	0.9984	0.1043
(9)	b_{27}=1.888E-7 (2.813E-8)	b_{28}=2.459492 (0.0146)	b_{29}=0.07792 (0.0149)	b_{30}=1.037102 (0.0135)	0.9987	0.0142
(10)	b_{31}=0.00001 (2.413E-6)	b_{32}=2.073132 (0.0228)	b_{33}=0.918631 (0.0247)	b_{34}=0.953745 (0.0180)	0.9974	3.3231

Eucalyptus nitens

Equation	**Parameter estimates**				***Adjusted R^2***	***RMSE***
(2)	b_0=23.23792 (11.4785)	b_1=-0.34626 (0.0586)	b_2= 0.70549 (0.0728)		0.8437	3.0194
(3)	b_3=0.000068 (0.000017)	b_4=1.936645 (0.0752)	b_5=0.800026 (0.0628)	b_6=1,005736 (0.0252)	0.9956	14.9311
(4)	b_7=0.000025 (2.157E-6)	b_8=2.24867 (0.0140)	b_9=0.665185 (0.0128)	b_{10}=0.980934 (0.00781)	0.9987	4.2858
(5)	b_{11}=0.000026 (4.245E-6)	b_{12}=2.353757 (0.0326)	b_{13}=0.08703 (0.0265)	b_{14}=0.991036 (0.0168)	0.9960	1.5209
(6)	b_{15}= 2.714E-6 (5.996E-7)	b_{16}=2.756195 (0.0409)	b_{17}=0.180144 (0.0308)	b_{18}=1.002181 (0.0218)	0.9941	1.1395
(7)	b_{19}=0.000231 (1.97E-5)	b_{20}=1.902716 (0.1489)	b_{21}=0.485519 (0.1429)	b_{22}=0.834961 (0.1109)	0.9475	14.9173
(8)	b_{23}= 4.196E-7 (3.662E-8)	b_{24}=2.24873 (0.0140)	b_{25}=0.667739 (0.0128)	b_{26}=0.980905 (0.00783)	0.9987	0.0734
(9)	b_{27}=4.219E-7 (7.089E-8)	b_{28}=2.355724 (0.0341)	b_{29}=0.089347 (0.0277)	b_{30}=0.99033 (0.0175)	0.9957	0.0256
(10)	b_{31}=0.000016 (2.892E-6)	b_{32}=1.844636 (0.0275)	b_{33}=0.93374 (0.0290)	b_{34}=0.973451 (0.0137)	0.9956	3.4338

Table 4. Equations for *dg* estimation from $\bar{d}$ for *Eucalyptus globulus* and *Eucalyptus nitens* plantations.

	Equation	Adjusted R^2	RMSE
Eucalyptus globulus	$dg = 1.0405 \cdot \bar{d} + 0.4067$	0.9954	0.5474
Eucalyptus nitens	$dg = 1.0322 \cdot \bar{d} + 0.344$	0.9937	0.4365

Table 5. Predicted yield for the two silvicultural alternatives considered.

	N_0=2400				N_0=1600			
	Eucalyptus globulus		*Eucalyptus nitens*		*Eucalyptus globulus*		*Eucalyptus nitens*	
N_1 (stems ha^{-1})	1700		2100		925		1300	
H_{01} (m)	27.6		27.2		28.5		28.7	
T (years)	14		11		15		12	
dg (cm)	16.7		16.8		20.3		20.2	
Yield units	ha^{-1}	ha^{-1} y^{-1}	ha^{-1}	ha^{-1} y^{-1}	ha^{-1}	ha^{-1} y^{-1}	ha^{-1}	ha^{-1} y^{-1}
V (m^3)	356.6	25.5	503.0	45.7	356.3	23.8	489.7	40.8
W (Mg)	204.1	14.6	236.3	21.5	208.2	13.9	244.6	20.4
W_w (Mg)	33.5	2.4	52.9	4.8	34.6	2.3	53.9	4.5
W_c (Mg)	24.8	1.8	25.5	2.3	24.9	1.7	28.0	2.3
C (Mg)	101.1	7.2	148.4	13.5	104.2	6.9	151.9	12.7
E (TJ)	3.430	0.245	4.000	0.364	3.501	0.233	4.141	0.345
E_w (TJ)	0.531	0.038	0.865	0.079	0.549	0.037	0.882	0.074
UC (Mg)	83.2	5.9	110.9	10.1	85.0	5.7	108.4	9.0

FIGURE CAPTIONS

Figure 1. Location of the sample plots. *Eucalyptus globulus* (triangles) and *Eucalyptus nitens* (squares).

Figure 2. Carbon accumulation in aboveground biomass and soil organic layer over time (Mg ha^{-1}) for *Eucalyptus nitens* and *Eucalyptus globulus* plantations.

Figure 3. Relation between average crown biomass and number of stems per hectare (*N*) for *Eucalyptus nitens* and *Eucalyptus globulus* plantations: determination of self-thinning threshold.

Figure 4. Stand Density Management Diagram for *Eucalyptus globulus* with isolines for: quadratic mean diameter, carbon in biomass and organic soil, Hart-Becking index, mortality and sample plots.

Figure 5. Stand Density Management Diagram for *Eucalyptus globulus* with isolines for: usable cellulose, aboveground biomass energy, harvest limits and mortality

Figure 6. Stand Density Management Diagram for *Eucalyptus nitens* with isolines for: quadratic mean diameter, carbon in biomass and organic soil, Hart-Becking index, mortality and sample plots.

Figure 7. Stand Density Management Diagram for *Eucalyptus nitens* with isolines for: usable cellulose, aboveground biomass energy, harvest limits and mortality.

Figure 8. Wood proportion in the stem in relation to quadratic mean diameter for both species.

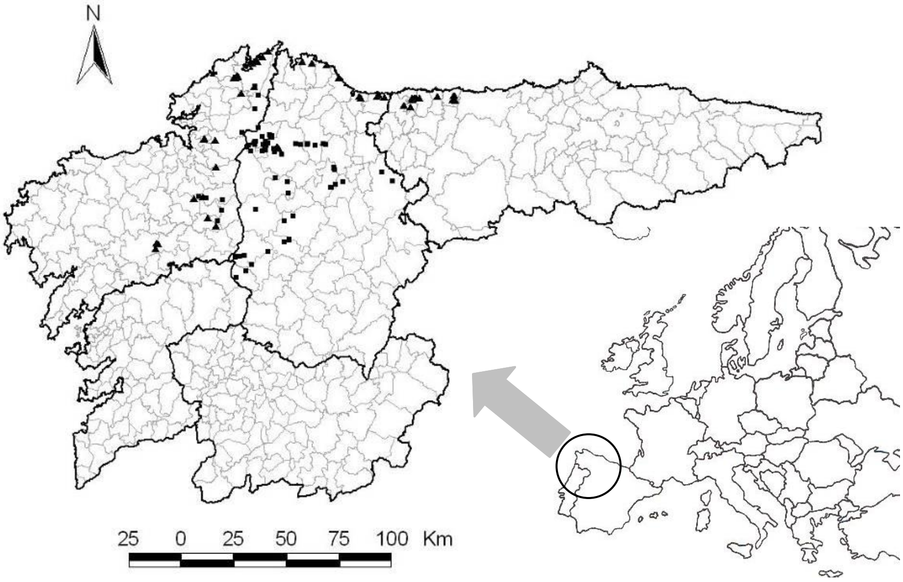

Figure 1. Location of the sample plots. *Eucalyptus globulus* (triangles) and *Eucalyptus nitens* (squares).

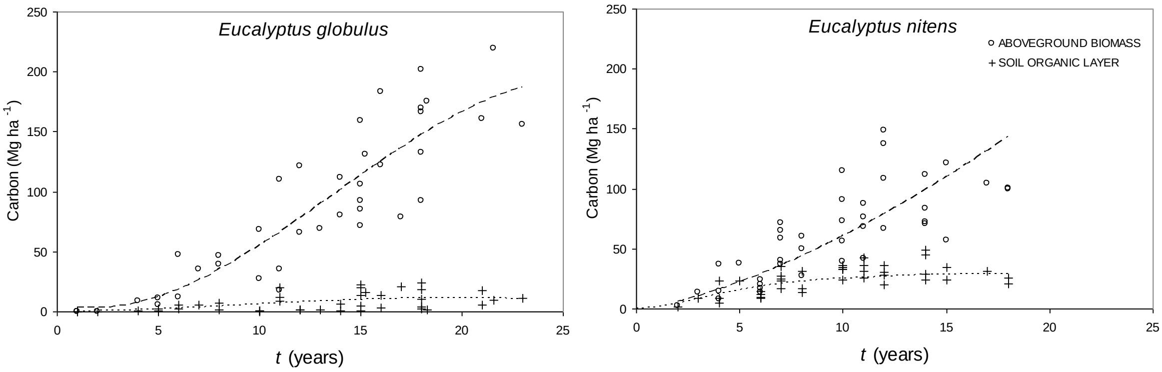

Figure 2. Carbon accumulation in aboveground biomass and soil organic layer over time (Mg ha^{-1}) for *Eucalyptus nitens* and *Eucalyptus globulus* plantations.

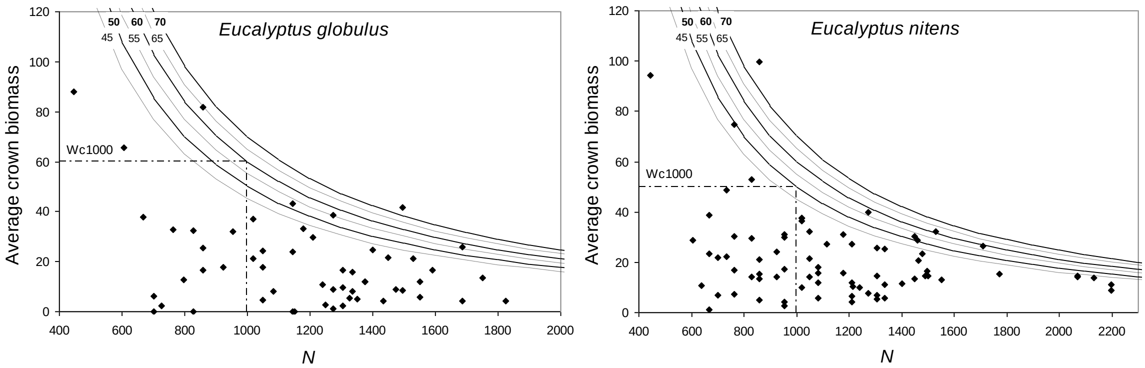

Figure 3. Relation between average crown biomass and number of stems per hectare (*N*) for *Eucalyptus nitens* and *Eucalyptus globulus* plantations: determination of self-thinning threshold.

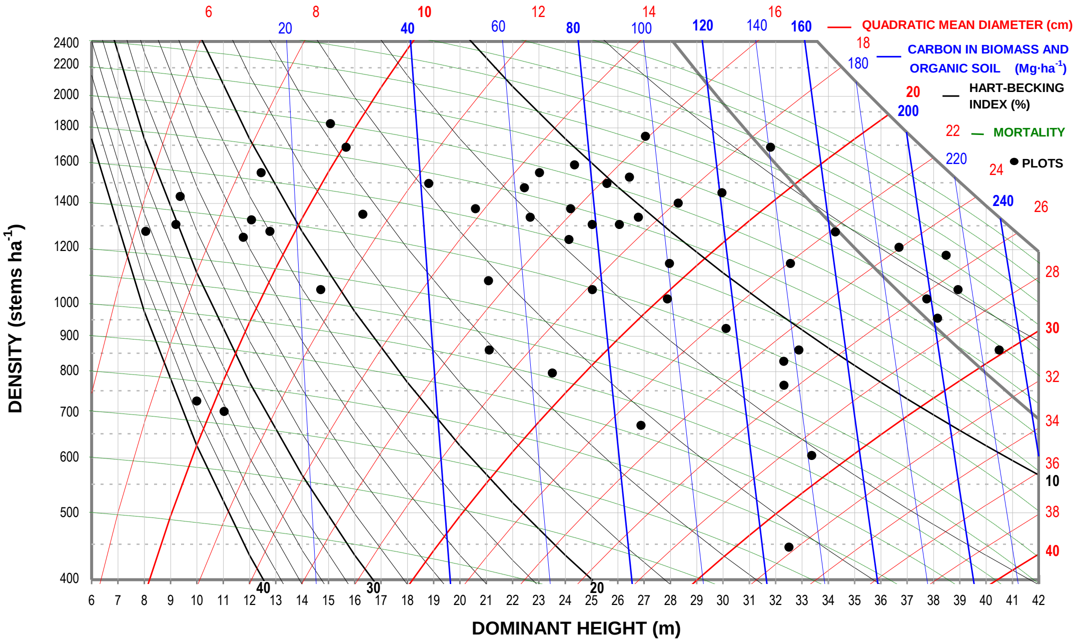

Figure 4. Stand Density Management Diagram for *Eucalyptus globulus* with isolines for: quadratic mean diameter, carbon in biomass and organic soil, Hart-Becking index, mortality and sample plots.

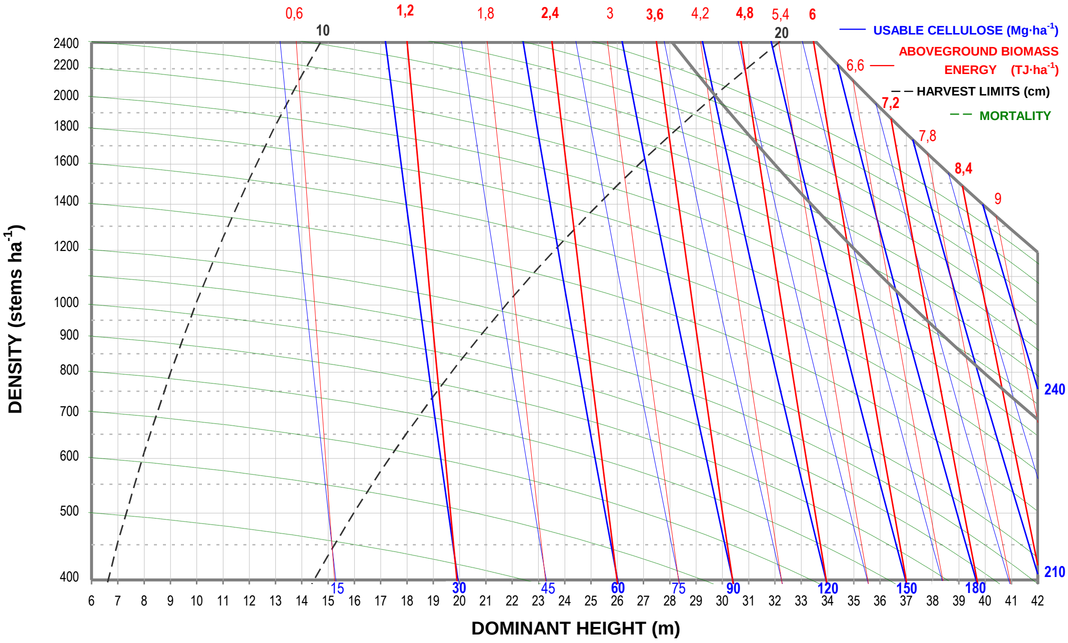

Figure 5. Stand Density Management Diagram for *Eucalyptus globulus* with isolines for: usable cellulose, aboveground biomass energy, harvest limits and mortality

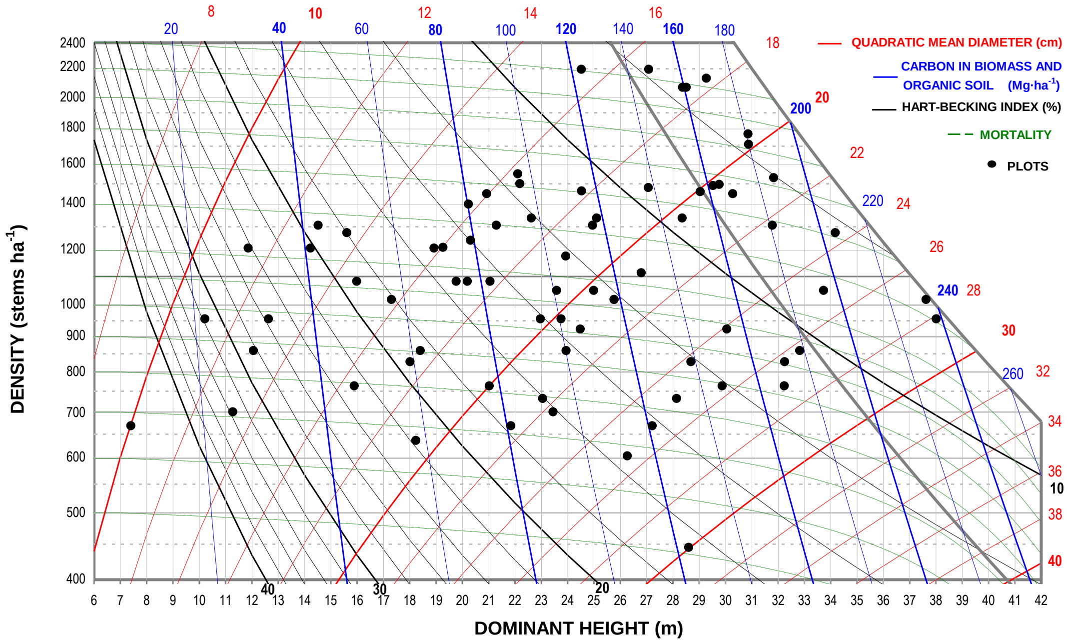

Figure 6. Stand Density Management Diagram for *Eucalyptus nitens* with isolines for: quadratic mean diameter, carbon in biomass and organic soil, Hart-Becking index, mortality and sample plots.

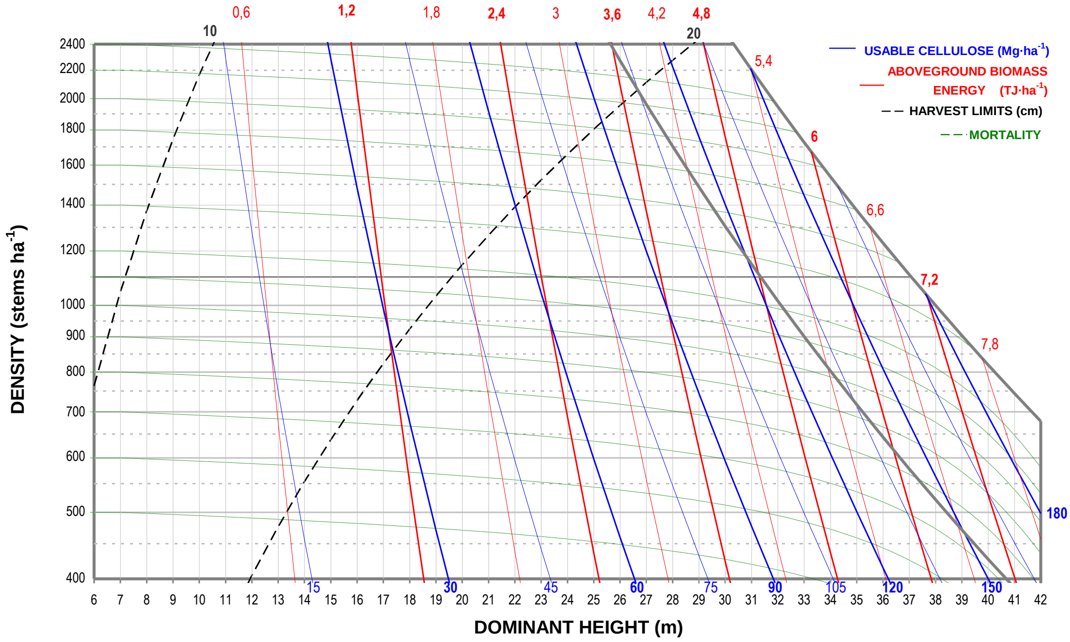

Figure 7. Stand Density Management Diagram for *Eucalyptus nitens* with isolines for: usable cellulose, aboveground biomass energy, harvest limits and mortality.

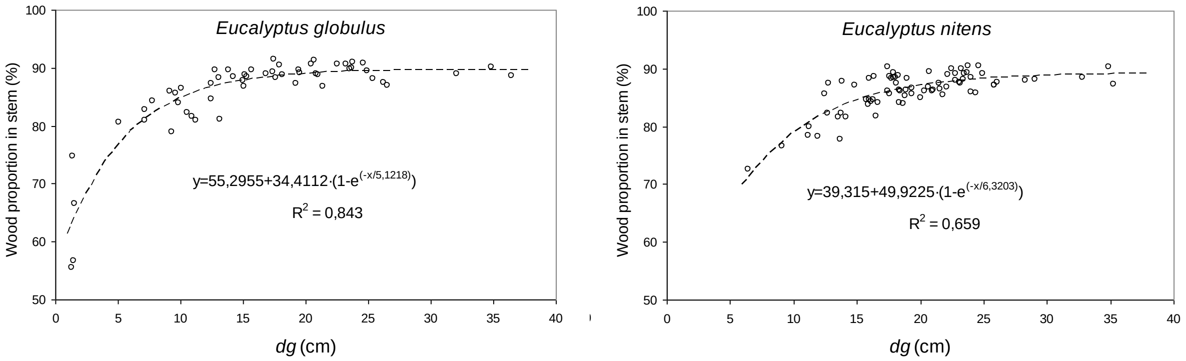

Figure 8. Wood proportion in the stem in relation to quadratic mean diameter for both species.